JOURNAL OF MATERIALS SCIENCE **40** (2005) 4911 – 4916

Computer simulation of the solidification of cast titanium dental prostheses

XIN-PING ZHANG*, GUANG CHEN
Department of Materials Science and Engineering, Nanjing University of Science and Technology, Nanjing 210094, P.R. China
E-mail: zxp_0517@163.com

SHOU-MEI XIONG, QIANG-YAN XU
Department of Mechanical Engineering, Tsinghua University, Beijing 100084

Temperature distributions in titanium dental castings and molds are of great influence on the quality of titanium dental castings, and few efforts have been made in the numerical simulation of heat transfer in the process for casting titanium for dental applications. A finite difference scheme of the component-wise splitting method, which is unconditionally stable, was developed to solve the three-dimensional heat transfer problem for titanium dental casting during the investment cast and centrifugal cast process. 4 kinds of runner system were simulated and the computational efficiency were analyzed by the component-wise splitting method and the explicit finite difference method, the results shown that the techniques used in the current research can greatly improve the computational efficiency of the simulation system. The porosity predictions of 4 kinds of runner system were carried out with the simulation program. The predicted results were in good agreement with those of literatures.

1. Introduction

Because of excellent biocompatibility, corrosion resistance, Ti and its alloys are increasingly being used in dental applications, such as dental crowns [1, 2], fixed [3] and removable partial dentures [4]. The investment casting process can offer the possibility of making near net shape castings with high dimensional accuracy and high casting quality, so with the help of centrifugal or vacuum-pressure mold filling techniques, investment casting is the most commonly used method of making such titanium dental prostheses [5–7]. However, porosity defects, which caused by volumetric shrinkage of alloy during the solidification process, are some of the most frequently occurring defects in titanium dental casting and are still of great concem [8–11]. Traditionally dental technicians often relied on practical experience and trial and error methods to determine the runner and gating systems to fabricate sound dental castings. However, their expertise did not extend to titanium which is especially susceptible to porosity.

The temperature distributions in the investment castings and molds are of great influence on the quality of the investment castings, so that many efforts have been made in solidification simulation of the investment casting process [12–17]. Numerical simulation techniques provide an effective way to study the solidification sequence of dental castings, but there are few reports on the computer simulation of casting process of titanium dental castings. Wu *et al*. used a commercial software package, MAGMASOFT, to numerical study shrinkage and gas porosity in dental castings, and an optimized running and gating system design was then experimentally cast, which resulted in porosity-free castings [18–21]. In current research work, a numerical simulation software of 3-D temperature field of titanium dental castings was developed with employing of the component-wise splitting method.

2. Materials and methods

2.1. Numerical simulation method

2.1.1. Component-wise splitting schemes for the heat conduction equation

Owing to the high filling rate on the centrifugal casting machine, the whole casting was filled in only ∼0.2 s During such a short filling process, no solidification occurred according the coupled fluid flow and heat transfer simulation [20]. In order to simplify the thermal analysis process, an "instant fill" assumption is made to the mold filling process. The thermal effect of the mold filling process is either neglected or considered accurately by an initial temperature distribution of the investment casting and the mold when the mold filling simulation is applied. Mathematically, the heat transfer problem during the investment casting process can be described by the following heat conduction equation in

* Author to whom all correspondence should be addressed.

an orthogonal coordinate system:

$$\frac{\partial T}{\partial t} - \alpha\left(\frac{\partial^2 T}{\partial x^2} + \frac{\partial^2 T}{\partial y^2} + \frac{\partial^2 T}{\partial z^2}\right) = 0 \qquad (1)$$

where $\alpha = \lambda/\rho c_p$ is the thermal diffusivity, ρ is the density, c_p is the specific heat, λ is the thermal conductivity, t is the time, T is the temperature, and x, y, z are the coordinate directions, respectively.

For the heat conduction problem, the following splitting scheme for Equation 1 can be obtained:

$$\begin{cases} \dfrac{T^{j+1/3} - T^j}{\tau} + \Lambda_x((1-\sigma)\cdot T^j + \sigma \cdot T^{j+1/3}) = 0 \\ \dfrac{T^{j+2/3} - T^{j+1/3}}{\tau} + \Lambda_y((1-\sigma)\cdot T^{j+1/3} + \sigma \cdot T^{j+2/3}) = 0 \\ \dfrac{T^{j+1} - T^{j+2/3}}{\tau} + \Lambda_z((1-\sigma)\cdot T^{j+2/3} + \sigma \cdot T^{j+1}) = 0 \end{cases} \qquad (2)$$

where σ is the weighting factor and with $\sigma = 0.5$, the scheme is absolutely stable and has a second-order approximation in τ and the whole order of accuracy of the scheme is O $(\tau^2 + h^2)$, where $h = \max(\Delta x, \Delta y, \Delta z)$. $\Lambda_x, \Lambda_y, \Lambda_z$ are the approximations for operators $A_x = -\alpha(\partial^2/\partial x^2)$, $A_y = -\alpha(\partial^2/\partial y^2)$, $A_z = -\alpha(\partial^2/\partial z^2)$, respectively, and $\alpha = \frac{\lambda}{\rho c_{\text{eff}}}$, where c_{eff} is the equivalent heat capacity when the latent heat release of the casting solidification is considered by the equivalent heat capacity method. Each equation in Equation 2 may be solved easily by a one-dimensional factorization (sweep) method.

2.1.2. Latent heat formulation

The way in which the evolution of latent heat during phase changes is described using the effective heat capacity method which can be expressed as follows:

$$c_{\text{eff}} = c_p - \rho L \frac{\partial f_s}{\partial t} \qquad (3)$$

where L the latent heat of the casting alloy and f_s the solid fraction of the titanium dental casting, which indicates the latent heat release mode and is usually treated as a linear function of the temperature. In reality, the values of f_s and c_p could be determined experimentally as any function of the temperature.

2.1.3. Method for predicting porosity defects

The direct simulation method, which is based on shrinkage theory of molten metal, is suitable for prediction of the porosity defects of centrifugal casting [16], so in this work the direct simulation method is used to predict porosity defects in titanium dental castings made using the centrifugal investment casting process. A detailed account of the direct simulation method is shown in literature [16].

2.1.4. Heat transfer coefficient

During the centrifugal investment casting process, the the heat transfer conditions between the different component geometries vary throughout the process and are represented using the following treatment:

$$-\lambda \left.\frac{\partial T}{\partial n}\right|_b = h_b(T_{b+} - T_{b-})|_b \qquad (4)$$

where n is the normal direction of the interface considered, h_b is the heat transfer coefficient of the interface, when at the casting-air or mold-air interface, h_b involves both the heat convection coefficient and the radiation coefficient, and T_{b+}, T_{b-} the temperatures at the two sides of the interface. A detailed account of the calculated way of h_b is shown in literature [22].

2.1.5. Geometry of titanium dental casting and initial condition

The geometry of a typical titanium dental casting were taken from the literature [21] as were a selection of four running systems. The initial boundary conditions published for pouring temperature (1700°C) and mold preheat temperature (500°C) were also used.

2.1.6. Materials

Commercially pure Ti was used for the casting numerical. The solidification range was taken as 1660–1667°C, the latent heat was taken as 396 kJ/kg. The temperature dependent density and the temperature dependent specific heat and thermal conductivity are shown in Table I [23, 24].

TABLE I The temperature dependent density, specific heat and thermal conductivity

	Temperature (°C)									
Property	20	100	200	300	400	500	600	900	1000	>1600
ρ (kg/m^3)	4506							4320	4300	4110
c_p (J/(kg°)C)	527	544	621	669	711	753	837	837	837	837
λ (W/(m°)C)	16.3	16.3	16.3	16.7	17.1	18	18	18	18	18

The density of the mold was taken as constant at 2830 kg/m^3, the specific heat capacity was taken as 600 kJ/(kg.°C), thermal conductivity was taken as 0.9 W/(m.°C).

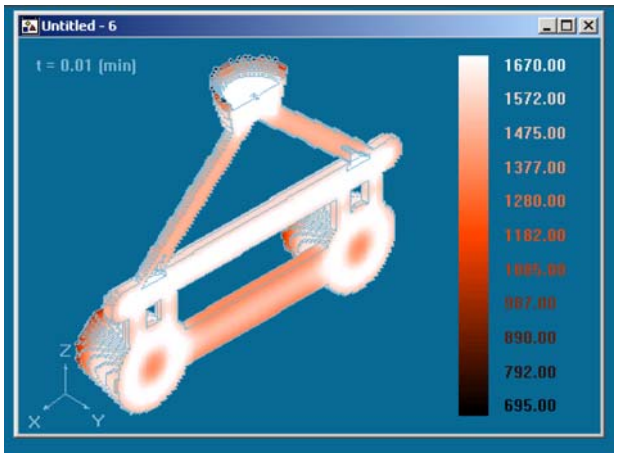

Figure 1 The temperature distribution in the tooth crown when the whole casting was 70% solidified: Design 1

3. Results

With the numerical basis of the component-wise splitting scheme and the technical considerations described above, a comprehensive three-dimensional thermal analysis software for titanium dental casting process was developed. The verification and application of the software are presented in this section.

3.1. Solidification process of titanium dental casting

Solidification isotherms of the Design 1 were shown when 70% of the casting is solidified in Fig. 1. White areas mean areas still in the liquid state; black areas show areas of 100% solidified Ti; and areas between liquidus temperature T_L and solidus temperature T_S are "mushy". The feeding path from the runner bar, which also acts as a reservoir for feed metal, to the tooth crown was blocked during the later stages of solidification at the narrowest section in the ingates.

The results of the calculation time and calculated solidification time of 4 kinds of runner system are shown in Table II. It is clear that the solidification times of titanium dental castings are very short, only one to two seconds, so a reasonable runner system is very important to fabricate a satisfactory tooth crown. The calculation times for the solidification simulation process was only 10–20 min which is acceptable to industry.

3.2. Shrinkage defects

The experimental result in the literature [18–21] and predicted results of porosity in t of Design 1 are shown in Fig. 2. The predicted results are in good agreement with the experimental ones.

By slicing through the casting model in small steps, it was found that most of the casting was well fed, but the simulations were carried out on the different designs, and the predicted results of Design 2, Design 3 and Design 4 are shown in Figs 3, 4 and 5. In the literature [18–21], for Design 2, Design 3 and Design 4 there are only the predicted results used MAGMASOFT commercial software package and no experimental results. In order to verify the component-wise splitting algorithm and techniques used in the simulation system, the shrinkage porosity predicted results in the literature [18–21] were shown in Figs 3(c), 4(c), and 5(b). In Design 2, no additional feeding measures were taken with only one large sprue being attached to each crown. Even though the diameter of the sprue was 5 mm, porosity was still indicated by the simulation at the sprue-crown junction (Fig. 3). Theoretically it would be possible to move the hot spot from this junction into the sprue by increasing the size of the sprue, but this was not practical, and therefore it was not carried out in the trial casting. In Design 3, there was still some shrinkage porosity in the vicinity of the ingate-crown junction (Fig. 4). Design 4 was the best Design, with no shrinkage porosity predicted in the casting by the simulation (Fig. 5). According to literature [18–21], in total 5 castings with Design 4 were experimentally cast, and no shrinkage or gas porosity was found in the castings. The computer predicted results compared well with the casting experiments.

3.3. Comparison of computational efficiency

In our prior works, a comprehensive three-dimensional thermal analysis software for investment casting process based on the explicit finite difference scheme was developed [16].In this paper, the computational efficiency of the two software was compared.

The grid number, grid size and time used for analysis of these castings were shown in Table II. It is clear that the techniques used in the current research can greatly improve the computational efficiency of the simulation system.

4. Discussion

4.1. Computational efficiency

In this work, a software was developed for the numerical simulation of solidification of titanium dental castings. Using the software, a 3-D solidification process can be

TABLE II Results of the calculation time and calculated solidification time of 4 kinds of runner system

No.	Size of cell (mm)	Number of liquid metal cells	Number of cells in the model domain	Solidification time (s)	Calculation time (min)		
					Implicit	Explicit	Explicit/Implicit
Design 1	0.4 × 0.4 × 0.4	60395	522444	1.7989	12	193	16.1
Design 2	0.4 × 0.4 × 0.4	53991	516040	2.4457	10	169	16.9
Design 3	0.4 × 0.4 × 0.4	59013	521062	1.9152	14	229	16.4
Design 4	0.4 × 0.4 × 0.4	67143	529192	2.1189	21	375	17.9

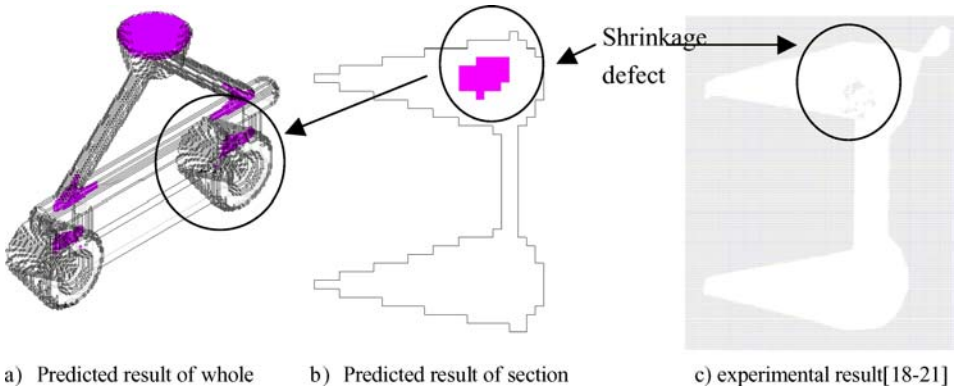

Figure 2 A comparison between our predicted results and experimentally determined results of Design 1.

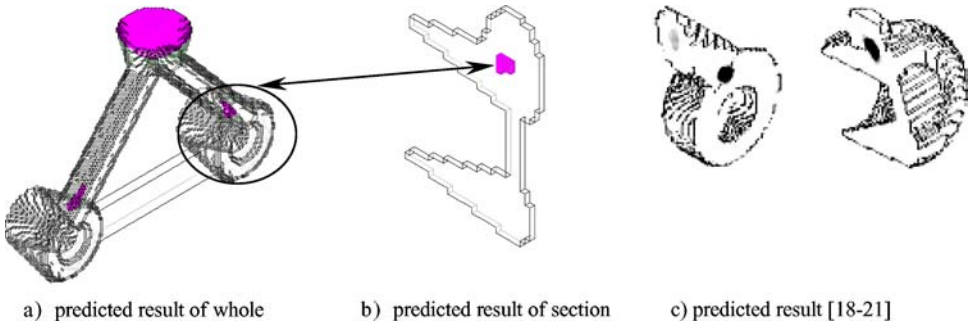

Figure 3 Comparison between our predicted results and those predicted results reported in the literature [18–21] of Design 2.

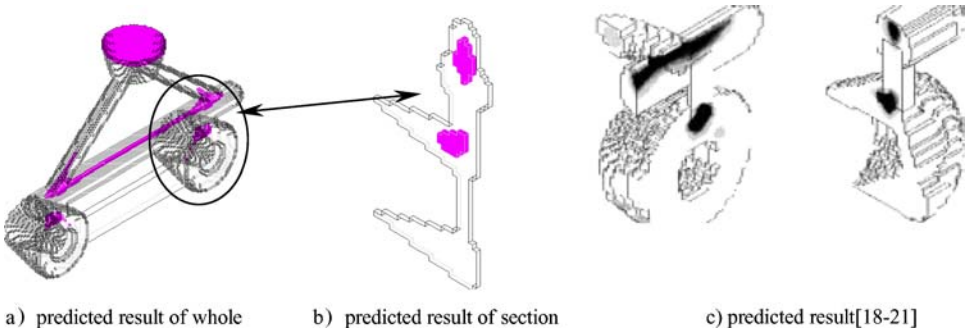

Figure 4 Comparison between our predicted results and those predicted results reported in the literature [18–21] of Design 3.

Figure 5 Comparison between our predicted results and those predicted results reported in the literature [18–21] of Design 4.

visualized, and the shrinkage defects in the titanium dental castings can be quantitatively predicted.

It is critical to the success of any metal casting process that the progress of solidification is controlled. To this end numerical modeling of heat transfer during solidification has become acceptable in the foundry industry. This is because it is possible to investigate the effects of alterations to the casting variables on final casting quality, without having to do costly trial-and-error experiments [25].

To obtain the numerical solution to the equation, the explicit finite difference method is used widely for its clarity and simplicity, but the main disadvantage of the method is its stability limitation for the time step τ, as

shown in the following expression:

$$\tau \leq \mathrm{MIN}\left[\frac{1/2\alpha}{1/\Delta x^2 + 1/\Delta y^2 + 1/\Delta z^2}\right] \quad (5)$$

where τ is the time step, Δx, Δy, Δz are the space steps in the x, y, z directions, respectively, α is the thermal diffusivity.

It is obvious that the maximum time step is limited by the thermal–physical properties and the minimum mesh size [22].

For a typical titanium dental investment casting component, very small mesh sizes should be used to obtain a better representation of the casting geometry since the thickness of the casting is usually small. To therefore, a very small time step should be used to meet the stability requirement for the explicit finite difference scheme, so that the computation time would be enormous to finish the solidification simulation process.

Since the component-wise splitting algorithm is absolutely stable, the time step may be amplified greatly than that of the explicit difference algorithm. In our prior work, the time steps of the component-wise splitting algorithm were greater over 100 times than those of the explicit algorithm, and the time used for analysis of the former were only 1/16 times of the latter. The techniques used in the current research can greatly improve the computational efficiency of the simulation system.

4.2. Porosity formation mechanism

Porosity defects are classified into gas porosity and shrinkage porosity defects. The former appears independently of solidification, the latter includes various type of defects that are classified into inner and outer shrinkage defects.

The formation mechanism or sequence of these porosity defects would be as follows:

(1) Gaseous elements, in particular hydrogen, are absorbed during melting and mold filling.
(2) Gas and oxides are entrapped during molding filling. The gas includes not only the air but also the gas generated on the mold. Gas bubbles or oxides float up due to the buoyancy force.
(3) Temperature and gas solubility decrease due to cooling, resulting in super-saturation. This can cause the gas porosity defect.
(4) When the melt temperature decreases below the liquidus temperature, solidification occurs, resulting in rejection of hydrogen in the liquid because of the lower partition coefficient of hydrogen. This leads to further super-saturation and pore growth.
(5) With developing the solid-liquid co-existing region (mushy region), solidification shrinkage causes shrinkage flow, resulting in pressure decrease due to the flow resistance. These causes pore and pore growth. At the same time, the solid phase morphology changes, namely the break-up and movement of solid phase occur. The liquid phase moves not only by the solidification shrinkage but also by the density difference caused by the segregation. The thermal expansion also causes the liquid flow.
(6) The pores grow with cooling and float up when they are large enough and the solid fraction is not so high, say less than 0.1.
(7) When the solid fraction exceeds a critical value, which is referred to as the critical solid fraction, the liquid cannot move and the pressure drastically decreases, resulting in pore nucleation and growth. Alternatively, it causes the depression of the outer side of casting. It also causes cracks in castings [16].

4.3. Porosity formation criteria

There are many methods to predict shrinkage defects, such as critical fraction solid method, temperature gradient method, Niyama's criterion $G/R^{0.5}$ method, equivalent liquid level falling method, hot spot allocation method, Oxide entrapment/hot spot allocation method and direct simulation method [22, 26, 27].

For the critical fraction solid method, the area surrounded by the region above a critical solid fraction g_{sc} where the liquid can hardly move, the degree of the defect can be evaluated from the volume of the region. Proper g_{sc} is selected depending on the kind of alloy and shape & size, and it is difficult to apply the case where a closed loop does not form.

For the temperature gradient method, the defect forms at the element where the maximum solid fraction or temperature gradient is below a critical value when the solid fraction reaches the critical solid fraction. Also the proper critical value is selected depending on the kind of alloy and shape & size, and it is difficult to apply the case where a closed loop does not form. It is used in case of eutectic alloys.

For the $G/R^{0.5}$ method, G is temperature gradient and R is cooling rate. The defect forms at the element where the maximum value of are below a critical value when the solid fraction reaches the critical solid fraction. The critical value does not change so much like other critical values.

For the hot spot allocation method, the total shrinkage volume is distributed to hot spots which are surrounded by layer with the critical solid fraction. Although it is basically the critical solid fraction method, it gives quantitative information.

For the oxide entrapment/hot spot allocation method, the total shrinkage volume is distributed to hot spots and the oxide entrapped elements. It can estimate the defect at elements except the hot spots but it is necessary to simulate the oxide entrapment.

Predict the porosity more quantitatively and accurately by considering the pressure decrease due to shrinkage flow, oxide entrapment, hydrogen diffusion for the direct simulation method. It is ideal but needs longer CPU and larger memory size.

Because the centrifugal force affects the porosity formation, so in the work the direct simulation method is used to predict the shrinkage defects of titanium dental casting fabricated by the investment casting with centrifugal technique.

5. Conclusions

(1) A finite difference scheme of the component-wise splitting method, which is unconditionally stable, was developed to solve the three-dimensional heat transfer problem for titanium dental casting during the investment cast and centrifugal cast process.

(2) The 4 kinds of runner system were simulated and the computational efficiency were analyzed by the component-wise splitting method and the explicit finite difference method, the results show that the techniques used in the current research can greatly improve the computational efficiency of the simulation system.

(3) The porosity predictions of 4 kinds of runner system were carried out with the simulation program. The predicted results were in good agreement with the predicted results found in the literature [18–21].

Acknowledgement

This research was financially supported by National Basic Research Program (G2000067208-3) and the Postdoctoral Foundation (20040350063).

References

1. M. ANDERSSON, B. BERGMAN and C. BESSING, *Acta Odontol Scand* **47** (1989) 278.
2. B. BERGMAN, C. BESSING and G. ERICSON, *ibid.* **48** (1990) 113.
3. T. JEMT and B. LINDEN, *Int. J. Periodontal Restor Dent* **12** (1992) 176.
4. R. BLACKMAN, N. BARGHI and C. TRAN, *J. Prosthet Dent* **65** (1991) 309.
5. E. P. LAUTENSCHLAGER and P. MONAGHAN, *Int. Dent. J.* **43** (1993) 245.
6. L. PRÖBSTER, J. GEIS-GERSTORFER and A. SIMONIS, *Dental Labor* **39** (1991) 1073.
7. E. BERG. *J. Dent.* **25** (1997) 113.
8. H. HERO, M. SYVERUD and M. WAARLI, *J. Mater. Sci.: Mater. Med.*, **4** (1993) 296.
9. *Idem.*, *Dental materials* **9** (1993) 15.
10. T. I. CHAI and R. S. STEIN, *J. Prosth Den.* **73** (1995) 534.
11. I. WATANABE, J. H. WATKINS and H. NAKAJIMA, *J. Dent. Res.* **769** (1997) 773.
12. F. SCHEPPE and P. R. SAHM, in "Modeling of Casting, Welding and Advanced Solidification Process IX," 2000, 207.
13. M. STEMMLER, G. LASCHET and L. HAAS, in "Modeling of Casting, Welding and Advanced Solidification Process IX," 2000 222.
14. W. D. GRIFFITHS, in "Modeling of Casting, Welding and Advanced Solidification Process IX," 2000 143–150.
15. G. WANG, L. YANG and T. Z. ZHOU, *J. Beijing Univ. Aeron. Astron.* **3** (2000) 249.
16. Z. J. LIANG, Q. Y. XU and J. T. LI, *Rare Metal Mater. Engng.* **3** (2003) 164.
17. M. WU, A. LUDWIG, P. R. SAHM and A. BUHRIG-POLACZEK, in "Modeling of Casting, Welding and Advanced Solidification Process IX," 2003, 261.
18. M. WU, J. SCHÄDLICH-STUBENRAUCH and M. AUGTHUN, *Den. Mater.* **14** (1998) 321.
19. M. WU, J. TINSCHERT and M. AUGTHUN, *ibid.* **17** (2001) 102.
20. M. WU, M. AUGTHUN and I. WAGNER, *J. Mater. Sci.: Mater. Med.* **12** (2001) 519.
21. M. WU, P. R. SANHM and M. AUGTHUN, *ibid.* **10** (1999) 519.
22. B. C. LIU and T. JING, in "Analog Simulation and Quality Control for Casting Engineering "(China Machine-9-Press, Beijing, 2001). (in Chinese).
23. Y. S. TOULOUKIAN, R. W. POWELL, C. Y. HO and P. G. KLEMENS, in "Thermophysical Properties of Matter: Thermal Conductivity-Metallic Elements and Alloys," The TPRC Data Series (4) 414.
24. Y. S. TOULOUKIAN, R. W. POWELL, C. Y. HO and P. G. KLEMENS, in "Thermophysical Properties of Matter: Thermal Conductivity-Metallic Elements and Alloys," The TPRC Data Series (4) 260.
25. O'MAHONEY DENIS and J.B. DAVID, *Experim. Therm. Fluid Sci.* **22** (2000) 111.
26. I. OHNAKA, A. SUGIYAMA and H. ONDA, in "Proceeding of Modeling of Casting and Solidification Processes VI," 2004, Taiwan.
27. J. R. SHENEFELT, R. LUCK, J. T. BERRYAND and R. P. TAYLOR, *Amer. Soc. Mechan. Eng., Manufact. Engng. Div., MED* **10** (1999) 507.

Received 27 October 2004
and accepted 1 February 2005